Proceedings of the 2022 IEEE
International Conference on Robotics and Biomimetics
December 5-9, 2022, Xishuangbanna, China

SWhegPro: A Novel Robust Wheel-Leg Transformable Robot

Cunxi Dai, Xiaohan Liu, Jianxiang Zhou, Zhengtao Liu, Zheng Zhu, and Zhenzhong Jia*

***Abstract*— This paper reports the design, implementation, and performance evaluation of SWhegPro, a swift and robust wheel-leg transformable robot that can operate under heavy payload. SWhegPro can shift wheel morphology between the wheel, e-shape leg, and S-shape leg, the corresponding gaits were developed and compared in simulation. The wheel/leg operation is driven by the same motor, so the actuation system and power can be utilized efficiently. Different from its predecessor which uses tendon-driven transformation mechanisms, SWhegPro utilizes self-locking electric push rods as transformation actuators. This makes it possible for SWhegPro to operate under heavy loads and is easier to repair. The robot was empirically built, and the design process, mechatronics infrastructure, and gait behavioral development were discussed. The performance of the robot was evaluated in various scenarios, including driving and turning in wheeled mode, step crossing, and irregular terrain passing in legged mode.**

I. INTRODUCTION

One of the most important performance indices for mobile robots is their terrain negotiability. Mobile robots are widely used in extreme environments that are dangerous for human to access. Terrains can be roughly divided into flat and rough terrains [1]. To achieve overall satisfactory performance, the robots need to balance energy efficiency and terrain negotiability. Generally, wheeled systems feature fast, smooth, and power-efficient locomotion on flat terrain, but behave poorly on rough terrain, which can result in large slip or even immobility [2]. In contrast, legged robots excel at negotiating rough terrain; however, they can hardly compare with wheeled robots in terms of speed and efficiency on flat ground [3]. Therefore, A hybrid wheel-leg transformable robot that takes full advantage of wheeled mobility on flat ground while employing legged mobility on rough terrains will likely have the best overall performance in various environmental conditions.

Hybrid Wheel-leg mobile platforms can be classified into three categories based on the hybrid strategy adopted, namely heteromorphic wheel robots, wheel-leg coexisting robots, and wheel-leg transformable robots. Heteromorphic wheel mechanism usually features wheels with specialized fixed-shapes. For example, Loper has four 3-spoke rimless wheels that perform well on both flat ground and stairs [4], [5]. RHex and ION utilize six compliant half-circle "C-shape" wheels (legs), also referred to as wheeled-legged (WHEG) mechanisms to overcome obstacles. Benefited from the curved shape and compliant spoke [6], [7], this C-shape leg behaves reliably with only open-loop control with lesser torque required compared to a straight stiff leg [8].

All authors are with the Shenzhen Key Laboratory of Biomimetic Robotics and Intelligent Systems, Department of Mechanical and Energy Engineering, Southern University of Science and Technology (SUSTech), Shenzhen, 518055, China. They are also with Guangdong Provincial Key Laboratory of Human-Augmentation and Rehabilitation Robotics in Universities, SUSTech, Shenzhen, 518055, China. *Corresponding author: jiazz@sustech.edu.cn

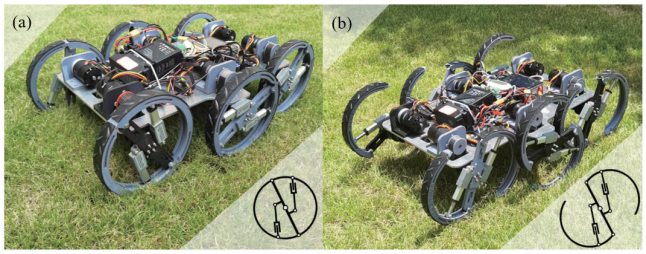

Fig. 1. SWhegPro, our wheel-leg transformable robot using electric push rods for mode switching between two main operation modes: (a) wheeled mode, and (b) legged mode. The figure also shows the corresponding schematics of the wheel-leg modules.

Another type of hybrid wheel-leg robot has a separate wheel and leg mechanism coexisting on the platform, and the locomotion is generated by the collaboration of these two mechanisms. Chariot III has two big wheels and four 3-DOF (degree of freedom) legs [9]. PEOPLER-II has two bars mounted on each of the four wheels, and its locomotion can switch between leg type and wheel type [10]. The hexapod RHex with one active rotational DOF on each half-circle leg can easily generate various legged behaviors via open-loop control [6]. The Whee-leg robot in [11] has two pneumatically actuated 3-DOF front legs and two independently driven rear wheels.

Different from the above robots, wheel-leg transformable robots feature transforming mechanisms that alter the morphology between wheels and legs. Some platforms utilize a passive 1-DOF mechanism that only transforms when encountering a vertical plane of the obstacle, such as wheel transformer, land devil ray, and shape-morphing wheel [4], [12], [13]. Some platforms use an active 1-DoF mechanism, and one of them uses origami to transform its wheel [8]. The 1-DOF mechanism can only be used to overcome a small range of obstacle sizes. Hence, to overcome this limitation, 2-DOF mechanisms have been investigated. The Quattroped and STEP are examples of platforms using 2-DOF mechanism [14], [15]. The Quattroped changes its wheel into the WHEG mechanism and moves the wheel up and down on the fly. This mechanism can be used to set a gait strategy to climb obstacles. Ref. [16] also proposes a Slegs design concept (without real experiments) using servo or linear actuator for mode switching; however, their design is extremely demanding on actuators and have serious flaws and limitations.

2022 IEEE International Conference on Robotics and Biomimetics (ROBIO) | 978-1-6654-8109-0/22/$31.00 ©2022 IEEE | DOI: 10.1109/ROBIO55434.2022.10011955

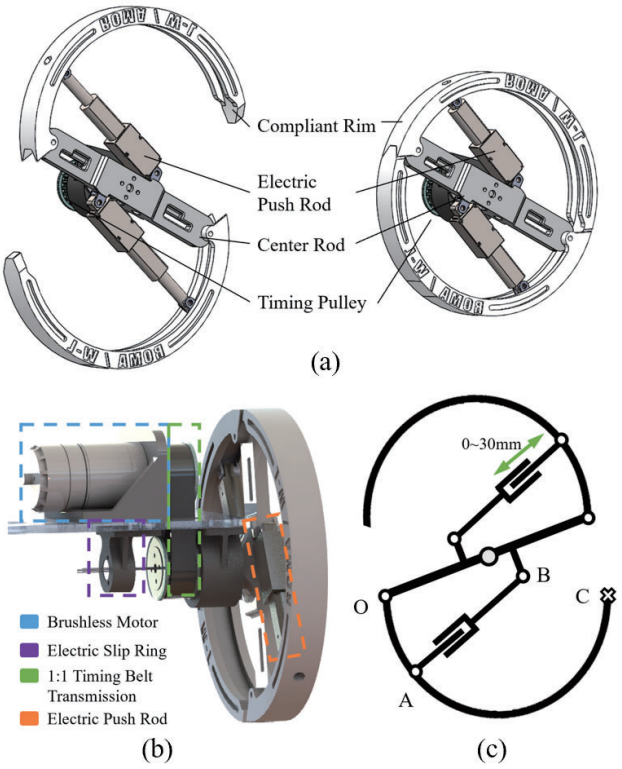

Fig. 2. Mechanical Design of the wheel-leg transformable module. (a) The mechanical structure of the wheel-leg transformable mechanism. (b) The composition of the wheel-leg module. (c) Schematic diagram of the module.

Previously, our group has developed a novel wheel-leg transformable robot SWheg with minimalist actuator realization [17]. The unique tendon-driven transformation mechanism allows a single central servo to drive the transformation of 4 or 6 wheel-leg modules simultaneously. Therefore, the same actuation system can be efficiently utilized in both wheeled and legged modes. The robot requires delicate calibration before operation because all modules share the same switching servo motor. The delicate transmission system in prototype robot might requires frequent repairing.

This paper introduces our newly developed, more robust wheel-leg transformable robot platform: SWhegPro, which is shown in Fig. 1. The 2-DoF wheel-leg transformation mechanism has been redesigned for three advantages: 1) the transformation mechanism forms a stable triangular structure to support the rim; 2) the on-wheel electric push rod allows the platform to operate with a much higher payload; and 3) allow the two rims on the same module to expand separately, resulting in more possible configurations and gaits.

II. SWhegPro Hardware Design

A. Transformable Wheel Module

In this study, we want to develop a robust wheel-leg transformable module that can be expanded to platforms with different leg configurations. Towards this goal, several design principles were utilized:

TABLE I
Robot Specifications

Length	Body	0.5m
	Hip-to-hip	0.21m
Width	Body	0.3m
	Leg-to-leg	0.3332m
Height	Body	0.154m
	Ground to hip (legged mode)	0.0965m
	Ground clearance (legged mode)	0.193m
Leg–wheel (i.e., rim) diameter		0.1m
Maximum radius of leg–wheel		0.1250m
Weight	Total	10.079kg
	Body	7.39kg
	Leg-wheel(each)	0.336kg
	Battery	0.673kg
Actuator	Driving	DJI M3508 motor(×6)
	Transformation mechanism	Electric Push Rod(×12)
Sensors	Encoder	(×6)@motor
	Temperature sensor	(×1)@computing unit
	Current measurement	(×1)@motor power output
	IMU	(×1)
	Battery voltage measurement	(×1)@power output
Battery	DJI TB48	30 min continuous run time

1) The wheel-leg module should be mechanically self-contained and only electrically connected to the robot platform.
2) The robot should be able to operate under a payload of three times self-weight.
3) The robot should feature self-lock maintaining wheeled and legged mode to avoid unnecessary power consummation.

In order to make the module mechanically self-contained and robust, we need to reduce the transmission mechanism complexity as much as possible. Therefore, we decided to place the transformation actuator on the wheel and drive the morphology change directly. We chose the electric push-rod to be the on-wheel transformation actuator based on two reasons. First is that the push-rod is non-backdrivable, and features self-locking in any position within its operation range. Second is that it is a self-contained actuator module so it is much easier to replace compared to SWheg, in which the whole tendon-driven network must be removed if the actuator requires repairing. These two properties allow the platform to operate under a much higher payload compared to SWheg and can maintain in different modes without extra actuator effort. A key problem to the on-wheel actuator is to prevent the wires from tangling while the wheel is rotating. In our design, we used an electrical slip ring to transmit electrical signals between on-wheel push rods and the robot's body. The placement of the slip ring is shown in Fig. 2(b).

As for the morphology in legged mode, we chose S-shaped was chosen to be similar to its predecessor SWheg and Turboquad [1], which showed outstanding performance on balancing terrain negotiation ability and motion smoothness of the platform. Towards the design goal of being robust, the transformation mechanism is designed to be a stable triangular structure with the center rod, electric push rod, and the base being the three sides. It has been observed that the compliant areas in fixed-shape legs like C-shaped and S-

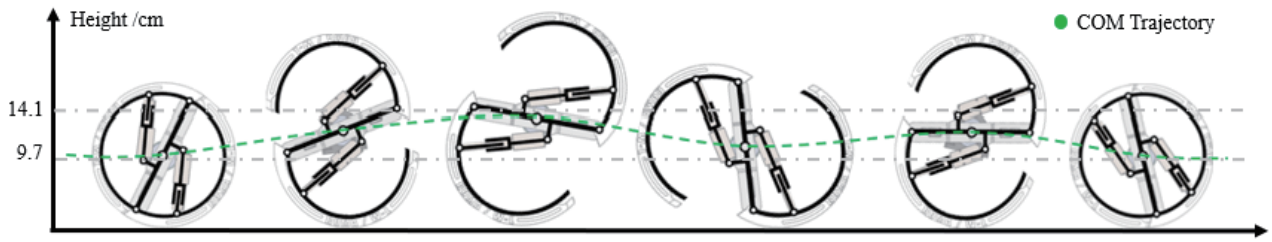

Fig. 3. Schematic time elapse of a single wheel-leg module transforming between wheeled mode and legged mode while advancing forward. The module center joint trajectory is marked, oscillating between 10cm and 14.1cm.

shaped legs [1] help the robot platform to be energy efficient and smooth in motion. Therefore, we want to maximize the compliant area in the leg-rim, i.e. the length of $\widehat{AC}$ shown in the schematic diagram in Fig. 2(c). The rim's radius is chosen proportional to the body size and, Based on these criteria, we set up the geometric model of the wheel is set up using MATLAB, and the specifications of the transformation mechanism design variables were chosen to maximize the compliant area in the leg-rim without causing mechanical interference. The center height variance during morphology transformation is shown in Fig. 3, oscillating between 10cm and 14.1cm.

We used a brushless motor with a 39:1 planetary reducer to drive the rotation of the wheel. The 1:1 transmission ratio using a timing belt. Note that the brushless motor is also a part of the module, driving both wheel and leg locomotion so the actuation system and power can be utilized efficiently. The 3D overview of the module is shown in Fig. 4(b).

B. Mechatronics Infrastructure

The main computation power on this robot is the Raspberry Pi 4B embedded computer, Robot Operating System(ROS) is used on this board for inter-module communication. 6 DJI M3508 brushless geared motors are used as the driving unit. And each motor is connected to a DJI C620 FOC controller. A socket can board that converts the USB signal to CAN signal is used to connect the FOCs and the embedded computer. 12 electric push rods are used as the actuators for wheel-leg transformation. The specifications of the robot are summarized in Table I.

III. Control and Simulation

A. Transformation Control

To obtain precise control over the transformation of the wheel-leg module, the kinematics of the transformation mechanism was simulated in MATLAB. The mapping between the push rod length and the transformation angle was used in control. The transformation angle θ_{trans} and coordinate setting is shown in Fig. 4, the linear kinematic mapping relationship is shown in the graph on the right side.

$$\begin{cases} \sqrt{{x_A}^2 + {y_A}^2} = 55 \\ \sqrt{(x_A - 98.4)^2 + (y_A + 21.5)^2} = l_{pushrod} \\ y_A < 0 \end{cases} \quad (1)$$

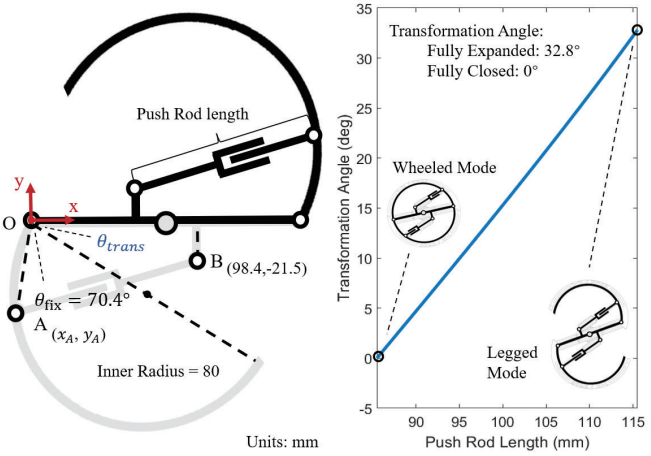

Fig. 4. Kinematic mapping between the length of the electric push rod and the transformation angle, marked in the left side.

$$\theta_{trans} = \begin{cases} \tan^{-1}\left|\frac{y_A}{x_A}\right| - \theta_{fix}, & x_A \geq 0 \\ 90 + \tan^{-1}\left|\frac{y_A}{x_A}\right| - \theta_{fix} & x_A < 0 \end{cases} \quad (2)$$

B. Wheeled Mode Motion

The control system consists of three layers: the instruction layer, planner layer, and behavior layer. The instruction layer processes high-level instructions, including control mode, walking gait, and moving speed. Control modes are managed by a finite state machine. During mode transitions, the position and control mode of joints will be adjusted accordingly. For now, the instructions are provided by a human operator. The desired speed, gait, and velocity are then sent to the controller of the corresponding mode. In the planner layer, the controller generates velocity/position trajectories for each joint according to the command. The behavior layer controls the actuators. The trajectory provided will be tracked by the actuators with PD controllers.

When the robot operates in wheeled mode, the control of the joints is straightforward. The rotation velocity (ω_i) of each joint is assigned based on the differential-wheel steering model. Joints on the same side of the robot will be assigned the same angular velocity, ω_{Left} or ω_{Right}, so the

As shown in Fig. 6 when the robot has a forward velocity $v_{desired}$ and a rotational velocity $\omega_{desired}$, its instant center of rotation will be located at point P_{ICR}. The turning radius can be expressed as:

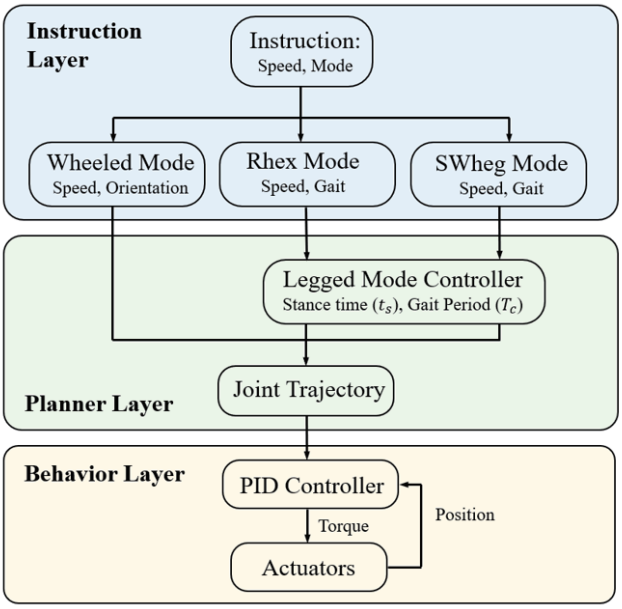

Fig. 5. Overall control structure.

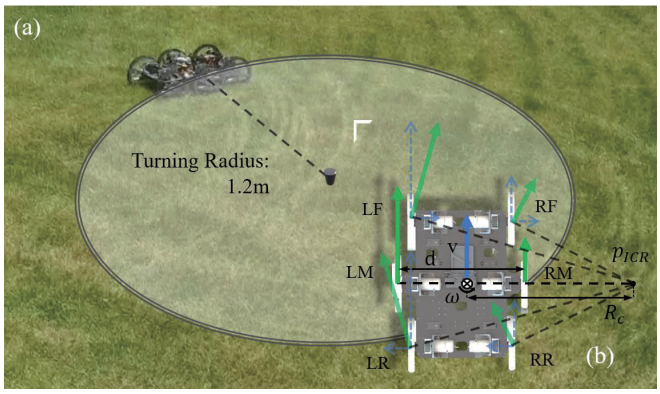

Fig. 6. Turning experiment on grass in wheeled mode. (a) Experiment photo with turning circle marked. (b) Differential-wheel steering model and the definition of wheel-legs.

$$R_c = \frac{v_{desired}}{\omega_{desired}} \tag{3}$$

Then, the angular velocity of joint on each side can be computed from

$$\omega_{Right} = \frac{v_{desired} + \frac{\omega_{desired} \cdot d}{2}}{R_{wheel} N_t} \tag{4}$$

$$\omega_{Left} = \frac{v_{desired} - \frac{\omega_{desired} \cdot d}{2}}{R_{wheel} N_t} \tag{5}$$

Where d is the width of the chassis and N_t is the speed reduction ratio. The wheeled mode control strategy can also be used in robot platforms with different leg configurations.

C. Legged Mode Motion

In legged modes, the planner-layer controller will generate a group of clock-driven periodic trajectories for joints. The trajectories generated are periodic functions of time, which have outputs ranging from 0 to 2π.

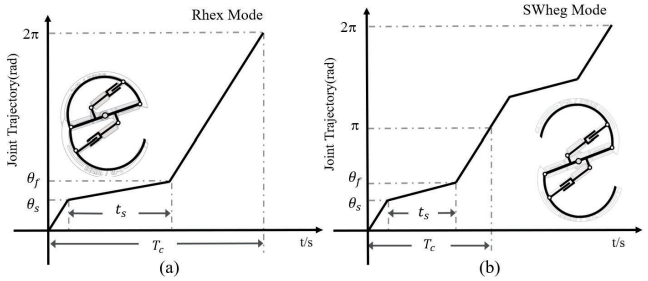

Fig. 7. Joint trajectory of legged modes. (a) Joint Trajectory of Rhex mode. (b) Joint Trajectory of SWheg mode.

For Rhex mode, the joint trajectory of walking mode has four key parameters: θ_s, θ_f, t_s and T_c.(See Fig. 7 (a).) T_c and t_s determine the ground speed a Leg, where T_c is the period of the function and t_s is the approximate stance time. θ_s and θ_f are geometric parameters of the leg. We suppose that the SWhegs approximately hit the ground when $\theta = \theta_s$ and leaves the ground when $\theta = \theta_f$.

The Joint trajectory of SWheg mode is similar to Rhex mode. Due to the symmetrical design of the SWheg module, the joint trajectory of $\pi < \theta < 2\pi$ repeats the trajectory of $0 < \theta < \pi$. (See Fig. 7 (b).)

By applying phase difference t_k to the legs, different gaits can be generated. This naive gait-generation method can be applied to both Rhex mode and SWheg mode. The following table shows the phase difference of some simple gaits and the corresponding gait diagram. The definition of Wheel-Leg modules can be found in Fig. 6 (b).

TABLE II
PHASE DIAGRAM

Gait Type	RF	RM	RR	LF	LM	LR
tripod	0	$\frac{1}{2}T_c$	0	$\frac{1}{2}T_c$	0	$\frac{1}{2}T_c$
ripple	0	$\frac{1}{3}T_c$	$\frac{2}{3}T_c$	$\frac{1}{6}T_c$	$\frac{1}{2}T_c$	$\frac{5}{6}T_c$

IV. PERFORMANCE EVALUATION

In this section, we do a lot of experiments to validate the motion performance of the SWhegPro.

A. Step Ascending Experiment

In this experiment, we tested the maximum step climbing height that SWhegPro can overcome in both Wheeled mode and SWheg mode. To increase the region of contact, the position of SWhegs on the same axis will be synchronized. The testing step was set up by decking 2.5cm boards (see Fig. 10(d).). The maximum step height SWhegPro can overcome in wheeled mode is 10cm, the same as the rim radius. In both Rhex mode and SWheg mode, the highest step the robot can overcome is 17.5cm. The pictures in Fig. 10(d) shows the step-climbing process in legged mode.

B. Motion Smoothness Experiment

This part of experiment is carried on Gazebo simulation platform. The parts of the robot model are generated from the original CAD file. The closed chain structure of the wheel

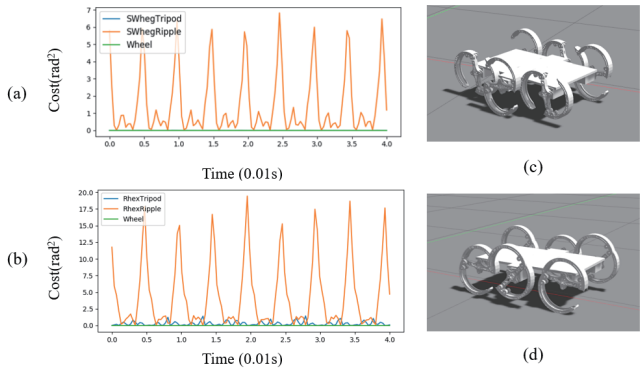

Fig. 8. Motion Smoothness Experiment. (a) Test results of Swheg mode. (b) Test results of Rhex mode. (c) Simulation model of SWheg mode. (d) Simulation model of Rhex mode.

mechanism is replaced with a 2-bar open chain structure in the simulation model.

We tested the different gaits on flat ground and collected the motion data. We use the change of orientation to evaluate the smoothness of motion. We installed an IMU on the chassis of the robot. The X-axis of IMU frame is parallel with the axes of the Wheels; the Z-axis points upward. The orientation of the robot is represented by a set of Z-Y-X Euler angle, ϕ, θ, ψ. Where ψ is the yaw, θ is the pitch, and ϕ is the roll. When the robot is operating on flat ground, the pitch and roll angle is supposed to be 0. So, the stability of motion is evaluated with a cost function, $J(\phi, \theta, \psi)$.

$$J(\phi, \theta, \psi) = K_s[\theta^2 + \phi^2] \tag{6}$$

Where K_s is a constant scaling factor. Here we take $K_s = 1000$. Fig. 8 shows the motion stability of SWhegPro on flat ground when using different gaits. In both Rhex mode and SWheg mode, the motion smoothness of ripple gait significantly underperforms tripod gait due to the lack of support. And in both gaits, SWheg mode is much more stable than Rhex mode. To sum up, the tripod gait of SWheg Mode has the best motion smoothness and was used in the field test.

C. Operation Under Payload

One of the prime design goals of SWhegPro is to operate under heavy payload, hence electric push rod featuring self-lock was chosen to be the transformation actuator. This experiment is to test the extreme payload the robot can handle while operating without failure. We chose sand to be the payload so weight can be continuously added, hence ensuring a more precise result. A set of extra fixtures was placed on top of the platform to prevent the sandbox from slipping. Pictures of the experimental setup are shown in Fig. 9. The robot can operate wheel-leg transformation under 12kg payload without breaking or clogging the actuator and can maintain a normal walking gait under 12kg payload. In wheeled mode, the robot can function under 15kg, heavier weight was not tested for the limit largely due to the structural strength of the parts instead of the actuator or geometries.

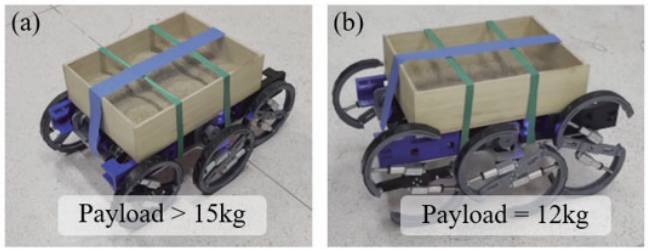

Fig. 9. Operation under payload, including wheel-leg transforming, moving in wheeled and legged mode.

D. Field Test

In this experiment, we measure the motion performance of SWhegPro over three different terrains: pebbles, grass and flat ground, as shown in the Fig. 10 (a)∼(c). Furthermore, we use the "specific resistance" to evaluate energy efficiency [18].

$$SR = \frac{P}{mgv} \tag{7}$$

The specific resistance is based on the robot's weight m, the average forward speed v, and the average power consumption P. We measured the power consumption directly from a power measurement module. Throughout all the field tests, the motion control parameters are set to the fixed values to ensure fair comparison between different modes. The joystick is only used to start or stop the robot's forward motion.

The test results are summarized in Table III and Table IV. Table III shows the test statistics which includes run times and failure rate. Hardware failure and deviation from course happened while traversing pebbles due to its harder surface and rougher terrain characteristic. Table IV shows the average forward speed, power, and the specific resistance of 5 runs over flat ground, grass, and pebbles for all tests. Some conclusions can be derived from Table IV:

1) SWhegPro moves well over three terrains, with speed variations range: $0.213m/s \sim 0.332m/s$ for wheeled mode and $0.196m/s \sim 0.282m/s$ for legged mode(tripod gait). In both modes, the forward speed over pebbles is the lowest due to pebble terrain's discontinuity and slippery characteristic. And the speed variation range of the legged mode is smaller than that of the wheeled mode because the discontinuity contact of the legged mode decreases the influence of terrains.
2) In both modes over three terrains, SWhegPro always consumes more energy at a faster speed. And it is more energy efficient while traversing flat ground compared to grass and pebbles. Moreover, SWhegPro features a lower SR value in wheeled mode compared to legged locomotion at a similar speed. The three terrains we selected in this experiment can all be classified into flat terrain categories, compared to steps and stairs being rough terrains. This shows that wheels are more energy efficient on flat terrains and hence is the ideal strategy when traversing flat terrains.

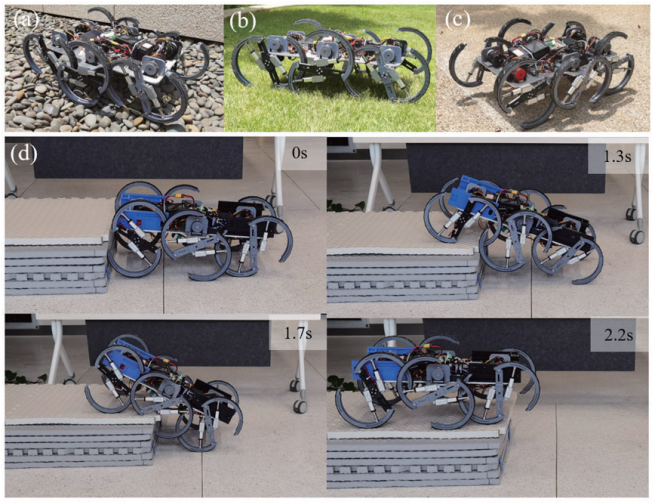

Fig. 10. Motion experiments on various terrains, (a) pebbles, (b) grass and (c) flat ground. (d) Pictures of overcoming 17.5cm step.

TABLE III
FIELD TEST STATISTICS

	flat ground	grass	pebbles
Total Number of Runs	10	10	10
Successful Runs	10	10	9
Hardware failures	0	0	1
Deviation from course	0	0	2

V. CONCLUSION AND FUTURE WORK

This paper reports the system design and performance validation of a novel wheel-leg transformable robot named SWhegPro. SWhegPro utilizes electric push-rods as actuators for transformation. Compared to its predecessor SWheg that uses tendon driven system, it is a more robust wheel-leg transformable robot designed for traversing various dangerous terrains and operating under heavy payload. We conducted both simulation and field experiments to evaluate its performance. The results show great mobility and obstacle negotiation capability. In the future, we will further improve the design to make the system more reliable. We will also improve the mode transition algorithm to enable faster and smoother movements. On the perception side, We will add depth camera and Lidar to enable the robot to classify and negotiate with different terrains by adjusting gaits and modes.

TABLE IV
VELOCITY AND ENERGY EFFICIENCY COMPARISON

		flat ground	pebbles	grass
wheeled mode	velocity(m/s)	0.332	0.213	0.287
	power(W)	20.475	13.423	17.857
	SR	0.623	0.638	0.629
tripod gait	velocity(m/s)	0.282	0.196	0.249
	power(W)	18.640	15.657	18.354
	SR	0.667	0.808	0.746

ACKNOWLEDGMENT

This work was supported in part by the Science, Technology and Innovation Commission of Shenzhen Municipality under grant no. ZDSYS20200811143601004.

REFERENCES

[1] W.-H. Chen, H.-S. Lin, Y.-M. Lin, and P.-C. Lin, "Turboquad: A novel leg–wheel transformable robot with smooth and fast behavioral transitions," *IEEE Transactions on Robotics*, vol. 33, no. 5, pp. 1025–1040, 2017.

[2] Y.-S. Kim, G.-P. Jung, H. Kim, K.-J. Cho, and C.-N. Chu, "Wheel transformer: A wheel-leg hybrid robot with passive transformable wheels," *IEEE Transactions on Robotics*, vol. 30, no. 6, pp. 1487–1498, 2014.

[3] R. Cao, J. Gu, C. Yu, and A. Rosendo, "Omniwheg: An omnidirectional wheel-leg transformable robot," *arXiv preprint arXiv:2203.02118*, 2022.

[4] L. Bai, J. Guan, X. Chen, J. Hou, and W. Duan, "An optional passive/active transformable wheel-legged mobility concept for search and rescue robots," *Robotics and Autonomous Systems*, vol. 107, pp. 145–155, 2018.

[5] C. F. Marques, J. Cristovao, P. U. Lima, J. Frazao, and R. Ventura, "Raposa: Semi-autonomous robot for rescue operations," in *2006 IEEE/RSJ International Conference on Intelligent Robots and Systems, IROS 2006, October 9-15, 2006, Beijing, China*, 2006.

[6] U. Saranli, "Rhex: A simple and highly mobile hexapod robot," *The International Journal of Robotics Research*, vol. 20, no. 7, pp. 616–631, 2001.

[7] S. P. Agrawal, H. Dagale, N. Mohan, and L. Umanand, "Ions: a quadruped robot for multi-terrain applications," *Int. J. Mater. Mech. Manuf.*, vol. 4, pp. 84–88, 2016.

[8] D. Y. Lee, S. R. Kim, J. S. Kim, J. J. Park, and K. J. Cho, "Origami wheel transformer: A variable-diameter wheel drive robot using an origami structure," *Soft Robotics*, vol. 4, no. 2, pp. 163–180, 2017.

[9] S. Nakajima, E. Nakano, and T. Takahashi, "Motion control technique for practical use of a leg-wheel robot on unknown outdoor rough terrains," in *International Conference on Intelligent Robots and Systems*, 2004.

[10] M. Kosugi, T. Ohya, and T. Migita, "Motion analysis with experimental verification of the hybrid robot peopler-ii for reversible switch between walk and roll on demand." *Chemischer Informationsdienst*, vol. 15, no. 11, pp. no–no, 1984.

[11] M. Lacagnina, G. Muscato, and R. Sinatra, "Kinematics, dynamics and control of a hybrid robot wheeleg," *Robotics and Autonomous Systems*, vol. 45, no. 3-4, pp. 161–180, 2003.

[12] Y.-S. Kim, G.-P. Jung, H. Kim, K.-J. Cho, and C.-N. Chu, "Wheel transformer: A miniaturized terrain adaptive robot with passively transformed wheels," in *2013 IEEE International Conference on Robotics and Automation*, 2013, pp. 5625–5630.

[13] S. Ryu, Y. Lee, and T. Seo, "Shape-morphing wheel design and analysis for step climbing in high speed locomotion," *IEEE Robotics and Automation Letters*, vol. 5, no. 2, pp. 1977–1982, 2020.

[14] S.-C. Chen, K.-J. Huang, W.-H. Chen, S.-Y. Shen, C.-H. Li, and P.-C. Lin, "Quattroped: a leg–wheel transformable robot," *IEEE/ASME Transactions On Mechatronics*, vol. 19, no. 2, pp. 730–742, 2013.

[15] Y. Kim, Y. Lee, S. Lee, J. Kim, H. S. Kim, and T. Seo, "Step: A new mobile platform with 2-dof transformable wheels for service robots," *IEEE/ASME Transactions on Mechatronics*, vol. 25, no. 4, pp. 1859–1868, 2020.

[16] S. Soyguder and W. Boles, "Slegs robot: development and design of a novel flexible and self-reconfigurable robot leg," *Industrial Robot: An International Journal*, vol. 44, no. 3, pp. 377–391, 2017.

[17] L. Zhengtao, D. Cunxi, L. Xiaohan, Z. Jianxiang, and J. Zhenzhong, "A hybrid wheel-leg transformable robot with minimal actuator realization," in *2013 IEEE International Conference on Advanced Robotics and Mechatronics*, 2013, pp. 5625–5630.

[18] G. V. T. Gabrielli, *What price speed? : specific power required for propulsion of vehicles*, 1950.